Multichannel polarization-entangled photon-pair source for entanglement distribution

Mengning Hu (胡梦宁), Yuping Chen (陈玉萍)*, Guangzhen Li (李广珍), and Xianfeng Chen (陈险峰)

State Key Laboratory of Advanced Optical Communication Systems and Networks, Department of Physics and Astronomy, Shanghai Jiao Tong University, Shanghai 200240, China

**Corresponding author: ypchen@sjtu.edu.cn*

Received December 11, 2015; accepted April 8, 2016; posted online May 20, 2016

A multichannel polarization-entangled photon-pair source in an MgO-doped periodically poled lithium niobate (MgO:PPLN) waveguide is proposed. Based on type I quasi-phase-matched spontaneous parametric down conversion in a single MgO: PPLN waveguide placed inside a Sagnac interferometer and pumped by monochromatic light, a source capable of supporting tens to hundreds of channels of polarization-entangled photon pairs in fiber communication bands simultaneously can be achieved. An inherent channel switch of this source is investigated, which will be significant for future entanglement distribution networks.

OCIS codes: 130.3730, 130.7405, 190.0190.
doi: 10.3788/COL201614.061301.

Tailored photonic sources suitable for producing entanglement constitute a basic constructional primitive in many quantum optics experiments in which they have been serving as a source of nonlocal correlations that violate Bell's inequalities[1] and in protocols for quantum information processing[2–5]. Due to its quantum feature, entanglement can neither be created nor increased by local operations and classical communications. Thus, the entanglement must be distributed to users by some physical means. A future quantum communication network can be realized by establishing entanglement distribution channels in addition to the classical communication channels[6]. Entangled photon pairs can be generated and distributed within these channels by an entanglement distributor. In order to take full advantage of fiber the transmission bandwidth, multichannel entangled photon pairs are being eagerly demanded. Obviously, it is not cost-effective to wavelength multiplex a large number of narrowband sources to realize multiple channels compared with that using a single multichannel source. Multichannel polarization-entangled photon-pair sources based on type II quasi-phase matching (QPM) spontaneous parametric down conversion (SPDC) in periodically poled lithium niobate (PPLN) waveguides have been reported[7]. But generally, few channels of entangled photon pairs can be produced. Actually, Lim *et al.* performed extensive research on wavelength division multiplexing and realized a wavelength-multiplexed entanglement distribution over an optical fiber, but it apparently cannot meet the demand for effective entanglement distribution[8,9].

In this work, we present a realizable switchable multichannel polarization-entangled photon-pair source based on type I QPM SPDC in an MgO:PPLN waveguide. It is potentially capable of simultaneously supporting tens to hundreds of independent wavelength channels in a fiber communication band with the current dense wavelength division multiplexing (DMDM) technology. In particular, an inherent dynamic tuning capability in this predicted source is presented here. The spectral emission rates of different wavelengths can be changed by adjusting the crystal temperature. It is a new way to tune the generation rate of the source in contrast to the method of tuning the pump power, which only changes the generation rate uniformly.

In periodically poled nonlinear crystals[10], such as PPLN and periodically poled potassium titanyl phosphate (PPKTP), the effective nonlinearity of the medium is periodically inverted by the application of an electric field with alternating directions during the crystal fabrication process. Periodically poled nonlinear crystals relax the phase-matching condition and allow a collinear configuration, where a much larger fraction of created photons can be entangled than in a cone-like geometry[11]. In some nonlinear crystals, such as PPLN and MgO:PPLN, the QPM condition is satisfied in a broad wavelength band owing to the intrinsic dispersion of the crystal[12–15].

Parametric down conversion can take place only when the energy conservation $\omega_p = \omega_s + \omega_i$ is satisfied, where the subscripts p, s, and i denote the pump, signal, and idler field, respectively. Consider the SPDC process in a z-cut, x-propagating MgO:PPLN with the length L. By the plane wave approximation, the pump field is described as $E_P = E_0 e^{i(k_p z - w_p t)}$. In the collinear case, the spectral emission rate per unit wavelength can be obtained by using Fermi's Golden Rules[16]:

$$R(\lambda_s) = \left[\pi G_1 E_0 L \,\mathrm{sinc}\left(\frac{L\Delta k}{2}\right)\right]^2 \frac{c}{n_s n_i \lambda_s^3 \lambda_i}, \qquad (1)$$

where n_s and n_i denote the refraction index of the signal and idler field, respectively, G_1 is the first-order Fourier coefficient of the quadratic nonlinear susceptibility $\chi^{(2)}(x)$,

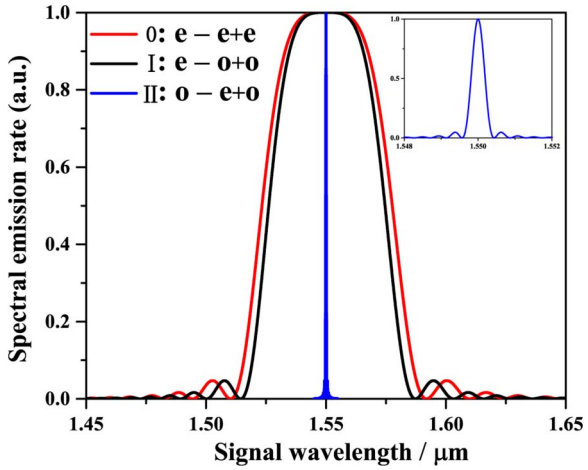

Fig. 1. Spectral emission rate of type I (black solid) and type II (red solid) QPM SPDC in a 2 cm-long 5% MgO:PPLN waveguide at the temperature of 20°C versus the signal wavelength. Curves of type 0, type I, and II have an FWHM of 54.3, 48.5, and 0.4 nm, respectively.

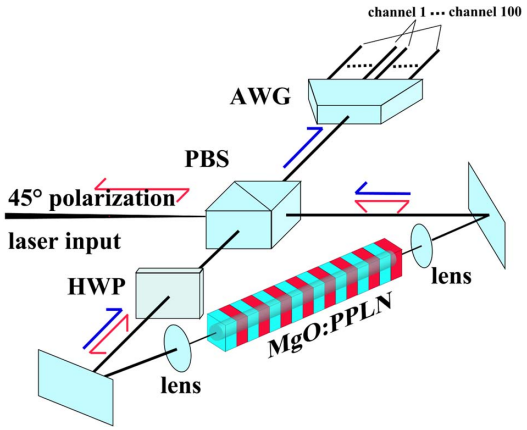

Fig. 2. Scheme of the proposed source. The red arrows show the propagation direction of the pump laser, and the blue arrows show that of the fiber communication band photon pairs created in the crystal.

which is a periodic function with the period Λ called the domain inversion period of the MgO:PPLN, and $\Delta k = \frac{n_p\omega_p}{c} - \frac{n_s\omega_s}{c} - \frac{n_i\omega_i}{c} - \frac{2\pi}{\Lambda}$. According to Eq. (1), photon pairs are generated efficiently when momentum conservation $\Delta k = 0$ is satisfied. Type 0 ($e \to e + e$), type I ($e \to o + o$), and type II ($o \to e + o$) QPM SPDC in MgO:PPLN were all studied, and appropriate poling periods were selected to guarantee the signal wavelength SPDC at 1550 nm correspondingly. It is noted that SPDC take place into the fundamental spatial mode for the signal, idler wavelength, and pump wavelength. The poling periods of type 0, type I, and type II QPM SPDC are 19.4, 19.8, and 8.6 nm, respectively. The results in Fig. 1 show that type 0 and type I QPM SPDC have broadbands of 54.3 and 48.5 nm, respectively, much broader than the broadband of 0.4 nm of type II QPM SPDC in a 2 cm-long 5% MgO:PPLN crystal.

By employing type I QPM SPDC in an MgO:PPLN waveguide, broadband polarization-entangled photon pairs can be generated in a bidirectional pumping arrangement[17]. Figure 2 shows the schematic of the multichannel polarization-entangled photon pair source, which is mainly composed of a broadband polarization-entangled photon-pair source and an arrayed waveguide grating (AWG). The MgO: PPLN crystal is placed at the center of the Sagnac interferometer. The polarization beam splitter (PBS) and the half-wave plate (HWP) function at both 775 nm and the fiber communication band. The diagonally polarized 775 nm monochromatic laser is separated into vertically and horizontal polarized components by the PBS. The HWP rotates the polarization of photons, passing through it by 90°C. Thus, the residual pump and telecom-band photon pairs are separated at the PBS automatically. Neglecting the phase difference between the photon-pair states generated by the two polarization components, the automatic combination of counter-propagating photon pairs at one output of the PBS produces the entangled state

$$|\psi\rangle = \int \mathrm{d}\omega \Phi\left(\frac{\omega_p}{2} + \omega\right) = (|\omega, H; -\omega, H\rangle + |\omega, V; -\omega, V\rangle), \tag{2}$$

where the complex function $\Phi(\omega)$ is the photon pair's spectral density, and $\Phi(\omega)\Phi^*(\omega) = R(\omega)$.

The AWG acts as a projector and usually is polarization and wavelength dependent. The combined output of the nth channel and $-n$th channel, with central frequencies $\frac{1}{2}\omega_p + \omega_n$ and $\frac{1}{2}\omega_p - \omega_n$, respectively, leads into the photo-pair state $|\psi\rangle = a_n|HH\rangle + b_n|VV\rangle$, where $a_n = \int \mathrm{d}\omega[\Phi(\frac{1}{2}\omega_p+\omega)f_n(\omega)f_{-n}(-\omega)+\Phi(\frac{1}{2}\omega_p+\omega)f_n(-\omega)f_{-n}(\omega)]$ and b_n is in the same form as $g_n(\omega)$ and $g_{-n}(\omega)$, $f_n(\omega)f^*_{-n}(\omega)$, and $g_n(\omega)g^*_{-n}(\omega)$ describe the probabilities that photons with frequency $\frac{1}{2}\omega_p + \omega$ can be coupled to the nth channel for H-polarization and V-polarization, respectively. They are probability functions with the maximum at the channel's central frequency $\frac{1}{2}\omega_p + \omega_n$. The maximum entangled state can be obtained when $a_n = b_n$. This condition is not realizable unless the probability functions are the same for different polarizations. Thanks to the current AWG technology, it is now possible to reduce the polarization dependence of the AWG[18]. Thus, with a specially designed AWG whose channel spacing is 25 GHz or less, a multichannel entangled photon-pair source with nearly 100 channels can be achieved, as shown in Fig. 2.

The refraction index of the MgO:PPLN crystal is temperature dependent, and in consequence, the spectral emission rate varies with temperature correspondingly. Thus, for a stable photon-pair generation rate, the crystal should be placed in a temperature controller to keep an appropriate working temperature. This temperature dependence feature also indicates that the generation rate of different channels could be changed in different

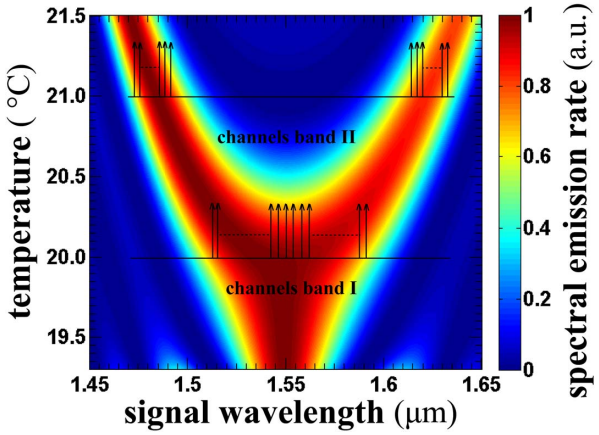

Fig. 3. Tuning curves of the photon pairs generation rate of type I QPM SPDC as a function of the crystal temperature in a 2 cm-long MgO:PPLN crystal. Two non-overlapping channel bands (black arrows) are supported at 20°C and 21°C.

proportions by adjusting the crystal temperature. Figure 3 shows the tuning curves of the spectral emission rate of type I QPM SPDC in a 2 cm-long MgO:PPLN crystal as a function of the crystal temperature. The generation rate of the central wavelength decreases, whereas that of sideward wavelengths increases when the crystal temperature rises. For instance, the generation rate of 1550 nm decreases from 1 to 0 as the crystal temperature rises from 20°C to 21°C, while those of 1500 and 1600 nm increase from 0 to 1. Some channels will be turned on or turned off at the corresponding temperature. The two bands that have a spectral emission rate greater than 0.5 at 20°C and 21°C are disjointed; therefore, they can be used as two-channel bands (Fig. 3). The two bands can be switched by tuning the crystal temperature. The channel band I is in state "on" at 20°C and in state "off" at 21°C, while channel band II shows an opposite trend. Thus, this source has an inherent channel switching function.

The generation rate for attaining a high visibility after distribution would be different for different pairs of users[5]. Although the tuning of the generation rate can be easily achieved by adjusting the pump power, it can only change the photon pairs' generation rate homogeneously rather than changing the shape of the spectral emission rate, and is far from the demand of achieving an optimal photon pair generation rate. Our proposed method to use temperature tuning to dynamically adjust the emission will therefore allow us to optimize the photon pair emission rates in different wavelength channels. Additionally, from an application point of view, both a broadband and a high generation rate are essential. Usually, there is a trade-off between the generation rate and bandwidth, for the amplitude of the spectral emission rate is proportional to L^2, while its half-width at half maximum is determined by $L\Delta k = 1.39$, where the sinc^2 function in Eq. (1) drops to 0.5. This means that Δk and the bandwidth are important to the generation rate, so we analyzed the relationships between them. Δk of type 0 (red solid

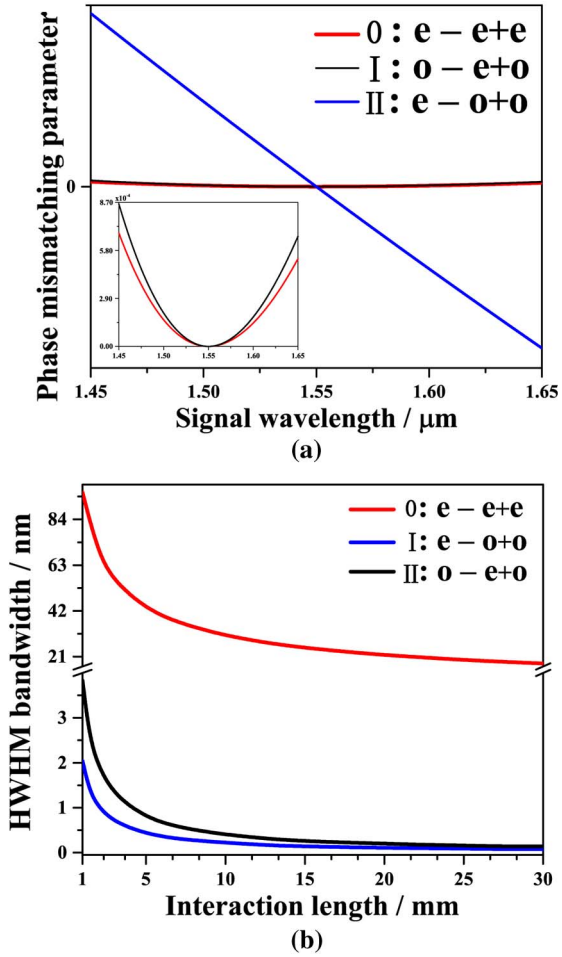

Fig. 4. Comparisons between QPM SPDC bandwidths of type 0, type I, and type II. The red, black, and blue solid lines represent type 0, type I, and type II, respectively. (a) The phase mismatching parameters as functions of the signal wavelengths of type 0, type I, and type II. (b) QPM SPDC bandwidths as functions of the interaction lengths of type 0, type I and type II.

line) and type I (black solid line) gently vary along with the emission wavelength changing, whereas Δk of type II (blue solid line) is significantly changed, which is due to the difference of the refractive indexes for the signal and idler photons. This suggests that the SPDC bandwidth of type II is much narrower than that of type I. Figure 4(b) demonstrates that as the interaction length gets longer, the SPDC bandwidth becomes narrower, and the bandwidth of type I is on the order of 10, which is much longer than the bandwidth of type II. For type I QPM SPDC, even with the long crystal length of 3 cm, the emission band is still broad enough (39.6 nm) to build a multichannel polarization-entangled photon-pair source with tens of channels.

In conclusion, a dynamically adjustable multichannel polarization-entangled photon-pair source based on type I QPM SPDC in MgO:PPLN pumped by a monochromatic laser is discussed theoretically. The source can provide polarization-entangled photon pairs suitable for fiber entanglement distribution in a broadband with theoretically

high spectrum brightness. The inherent channel switch of our source is found, which makes it possible to switch between different channels by adjusting the crystal temperature and also contributes to achieving an optimal generation rate for each channel to achieve a high visibility.

This work was supported by the National Natural Science Fund of China (Nos. 11574208, 10874120, and 60407006) and the Scientific Research Foundation for the Returned Overseas Chinese Scholars, State Education Ministry.

References

1. Z. Y. Ou and L. Mandel, Phys. Rev. Lett. **61**, 50 (1988).
2. C. H. Bennett, G. Brassard, C. Crépeau, R. Jozsa, A. Peres, and W. K. Wootters, Phys. Rev. Lett. **70**, 1895 (1993).
3. C. H. Bennett and S. J. Wiesner, Phys. Rev. Lett. **69**, 2881 (1992).
4. A. K. Ekert, Phys. Rev. Lett. **67**, 661 (1991).
5. X. Song, H. Li, C. Zhang, D. Wang, S. Wang, Z. Yin, W. Chen, and Z. Han, Chin. Opt. Lett. **13**, 012701 (2015).
6. H. C. Lim, A. Yoshizawa, H. Tsuchida, and K. Kikuchi, Opt. Express **16**, 14512 (2008).
7. S. Gao and C. Yang, Opt. Lett. **32**, 2653 (2007).
8. H. C. Lim, A. Yoshizawa, H. Tsuchida, and K. Kikuchi, Opt. Express **16**, 22099 (2008).
9. H. C. Lim, A. Yoshizawa, H. Tsuchida, and K. Kikuchi, Opt. Fiber. Technol. **16**, 225 (2010).
10. J. A. Armstrong, N. Bloembergen, J. Ducuing, and P. S. Pershan, Phys. Rev. **127**, 1918 (1962).
11. P. G. Kwiat, K. Mattle, H. Weinfurter, A. Zeilinger, A. V. Sergienko, and Y. Shih, Phys. Review. Lett. **75**, 4337 (1995).
12. N. E. Yu, J. H. Ro, M. Cha, S. Kurimura, and T. Taira, Opt. Lett. **27**, 1046 (2002).
13. M. H. Chou, K. R. Parameswaran, M. M. Fejer, and I. Brener, Opt. Lett. **24**, 1157 (1999).
14. C. Q. Xu, H. Okayama, and M. Kawahara, Appl. Phys. Lett, **63**, 3559 (1993).
15. M. Xia, J. Li, Y. Hu, W. Sheng, D. Gao, W. Pang, and X. Zheng, Chin. Opt. Lett. **13**, 113001 (2015).
16. A. Ling, A. Lamas-Linares, and C. Kurtsiefer, Phys. Rev. A **77**, 043834 (2008).
17. F. König, E. J. Mason, F. N. C. Wong, and M. A. Albota, Phys. Rev. A **71**, 033805 (2005).
18. X. Leijtens, B. Kuhlow, and M. Smit, *Arrayed waveguide gratings* (Springer, 2006).